Secondary Quinone in Photosystem II of *Thermosynechococcus elongatus*: Semiquinone−Iron EPR Signals and Temperature Dependence of Electron Transfer†

Christian Fufezan,*,‡,§ Chunxi Zhang,‡,|| Anja Krieger-Liszkay,§ and A. William Rutherford‡

Service de Bioénergétique, DBJC, CNRS URA 2096, CEA Saclay, 91191 Gif-sur-Yvette, France, and Institut für Biologie II, Biochemie der Pflanzen, Universität Freiburg, Schänzlestrasse 1, 79104 Freiburg, Germany

Received May 27, 2005; Revised Manuscript Received July 3, 2005

ABSTRACT: The secondary quinone acceptor, Q_B, has been studied in photosystem II (PSII) isolated from *Thermosynechococcus* (*T.*) *elongatus.* Thermoluminescence indicated that Q_B was present in this preparation. An EPR signal observed at low temperature at $g = 1.9$ was attributed to $Fe^{2+}Q_B^-$ on the basis of the characteristic period-of-two variations in its intensity depending on the number of laser flashes given at 20 °C. When samples showing the $Fe^{2+}Q_B^-$ signal were illuminated at 77 K, an EPR signal at $g = 1.66$ appeared with an amplitude proportional to that of the $Fe^{2+}Q_B^-$ signal. This signal is attributed to the $Q_A^-Fe^{2+}Q_B^-$ state. While these attributions have been made previously in PSII from other origins, they have remained relatively tentative since the characteristic period-of-two oscillations of Q_B had not previously been observed. The flash experiments indicated that more than one exchangeable plastoquinone is associated with the isolated PSII. The $g = 1.66$ signal from the $Q_A^-Fe^{2+}Q_B^-$ state was used to study the temperature dependence of electron transfer between the two quinones. Electron transfer occurred in half of the centers (after 30 s incubation) at −28 °C for Q_A^- to Q_B but at −58 °C for Q_A^- to Q_B^-. This marked difference for the two electron transfer reactions indicates different types of rate-limiting reactions. In the better studied but homologous system, the purple bacterial reaction center, the Q_A^- to Q_B step is limited by a gating process, while the Q_A^- to Q_B^- step is limited by protonation events. Similar reactions in PSII could give rise to the observed temperature dependence.

Photosystem II (PSII)[1] is the light-driven enzyme of photosynthesis in which electrons are taken from water and transferred over a chain of redox cofactors to plastoquinone (*1*, *2*). The protein forms two binding sites for quinones. These two quinones act as sequential electron acceptors and are known as Q_A and Q_B. Although these are both plastoquinones, their physical and chemical properties differ. Q_A is tightly bound and acts as a one-electron carrier, with a short-lived semiquinone state that undergoes no observable protonation events during its lifetime (*1*, *3*). Q_B acts as a two-electron and two-proton acceptor with a stable semiquinone intermediate, Q_B^- (*4*, *5*). While the Q_B^- semiquinone state is tightly bound, its quinone and quinol forms are exchangeable with the quinone pool in the membrane (*6*, *7*).

The photochemical reaction center of PSII is very similar to that in purple bacteria, and this is particularly marked for the electron acceptor side (*1*, *2*, *8*−*10*). In both systems a high-spin, non-heme ferrous ion is located between Q_A and Q_B, and the semiquinone radicals are magnetically coupled to the Fe^{2+} ion, giving rise to broad EPR signals with turning points around $g = 1.8$ and 1.9 (*1*, *2*, *11*, *12*).

In the purple bacterial reaction center the electron transfer between Q_A and Q_B and the associated protonation reactions have been studied in great detail (for reviews see refs *13* and *14*). In PSII the equivalent reactions have been the subject of numerous kinetic studies using sensitive light emission methods to probe the reactions occurring in the reaction center, in most cases while still in its native membrane rather than in isolated complexes (e.g., refs *15*−*19*). Few studies of Q_B and Q_B^- have been done on isolated complexes, and this has meant that studies of Q_B using direct spectroscopic methods are rare. This situation is at least partially attributable to the fact that preparations of PSII-enriched membranes (e.g., ref *20*), the most common material of study and the material that represents the first step in the preparation of more purified PSII from plants, rarely show typical Q_B activity.

Among the rare EPR studies to have dealt with Q_B^-, an $Fe^{2+}Q_B^-$ signal has been reported around $g = 1.94$ (*21*−*23*), a somewhat higher *g*-value than is usually attributed to $Q_A^-Fe^{2+}$ (24). In addition, a signal at $g = 1.66$, which had originally been associated to $Q_A^-Fe^{2+}$ (*25*), was subsequently reassigned to $Q_A^-Fe^{2+}Q_B^-$ (*23*, *26*). For the $g = 1.94$ signal,

† C.Z. was supported by a grant from the DRI of the CEA. C.F. was supported by a Marie Curie Training Site SPECBIO. The research was also supported by EU network INTRO2.

* Address correspondence to this author. Tel: ++33-(0)1.69.08.8657. Fax: ++33-(0)1.69.08.8717. E-mail: christian@fufezan.net.

‡ CNRS URA 2096.

§ Universität Freiburg.

|| Current address: Photochemistry Laboratory, Center for Molecular Science, Institute of Chemistry, The Chinese Academy of Sciences, Zhongguancun, Beijing 100080, P. R. China.

[1] Abbreviations: PSII, photosystem II; Q_A, primary quinone acceptor; Q_B, secondary quinone acceptor; FCCP, carbonyl cyanide 4-(trifluoromethoxy)phenylhydrazone; cyt b_{559}, cytochrome b_{559}; ChlZ, the redox-active chlorophyll; Car, redox-active β-carotene; TyrZ, redox-active tyrosine Y161 of the D1 protein; TyrD, redox-active tyrosine Y160 of the D2 protein; S_0, S_1, S_2, and S_3, redox states of the water oxidizing enzyme.

10.1021/bi051000k CCC: $30.25
Published on Web 09/02/2005

its original attribution to $Fe^{2+}Q_B^-$ was based on experiments in which this signal appeared when samples containing $Q_A^-Fe^{2+}$ (formed by illumination at low temperature) were warmed to a temperature where electron transfer from Q_A^- to Q_B was expected to occur, leading to a relatively stable Q_B^- state (*21*, *22*). In the work of Hallahan et al. (*23*) the assignment was based on the stability of the signal and a correlation with the $g = 1.66$ signal which had already been attributed to $Q_A^-Fe^{2+}Q_B^-$ (*26*). The assignment of the $g = 1.66$ signal as $Q_A^-Fe^{2+}Q_B^-$ was based on several arguments derived from the results of pretreatments of the sample that were assumed to affect the Q_B^- concentration. Perhaps the strongest of these arguments was a redox poising experiment that showed that the $g = 1.66$ signal could be generated over a range of potentials that was consistent for that expected for Q_B^- (*26*). While these arguments are reasonable, correlations with other Q_B^- related phenomena have yet to be made and the more definitive period-of-two behavior, which is the hallmark of Q_B function (*4*, *5*), has yet to be demonstrated. Thus the assignments for these signals, while reasonable, remain less than definitive.

In the literature there are several indications that PSII preparations from cyanobacteria maintain more functional Q_B than is generally found in preparations from higher plants (*25*−*28*). In the present work we have investigated the semiquinone−iron signals in PSII of *Thermosynechococcus elongatus*, the material that is currently the center of attention because it has provided the first crystallographic models (*10*, *29*). We have identified EPR signals associated with Q_B^- and used them to investigate the temperature dependence of electron transfer between the quinones in this preparation.

MATERIALS AND METHODS

T. elongatus (43-H strain) (*30*) cells were grown as described earlier (*31*). Purification of the PSII complex from this strain was essentially as described by Kirilovsky et al. (*32*) except that the detergent concentration for the washing steps of the column was 0.03%. Samples were finally resuspended in 40 mM Mes, pH 6.5, 15 mM $MgCl_2$,15 mM $CaCl_2$, and 1 M betaine. The O_2 evolving activity measured in a Clarke electrode was ∼3000 μmol of O_2/(mg of Chl·h) using 50 μM DCBQ (2,5-dichloro-1,4-benzoquinone) as an electron acceptor dissolved in ethanol.

Thermoluminescence was performed on PSII particles at a concentration of 40 μg/mL on a laboratory-build apparatus as described by Ducruet (*33*). Samples were dark-adapted for 3 min at 20 °C. Excitation flashes were also given at 20 °C followed by rapid cooling to −18 °C. Thermoluminescence was recorded with a heating rate of 0.5 °C s^{-1} up to 80 °C.

Low-temperature continuous wave (cw) EPR measurements were done using a Bruker 300 spectrophotometer equipped with an Oxford-900 liquid helium cryostat and ITC-503 temperature controller (Oxford Instruments Ltd.) and a standard Bruker cavity ST4102. Instrument settings were microwave frequency 9.4 GHz, modulation frequency 100 kHz, and as indicated in the figure legends. The samples for EPR were adjusted to 0.4−1 mg/mL, and 150 μL aliquots were loaded into quartz EPR tubes (Wilmad, 707-SQ-250M). Dark adaptations were done at room temperature for 10 min (short dark adaptation) or 15−24 h (long dark adaptation). The EPR samples were frozen and degassed with argon at 77 K and then thawed. Samples were handled in complete darkness. Flashes were given with a frequency-doubled Nd:YAG laser (Spectra Physics, 7 ns fwhm, 550 mJ) at room temperature. A frequency of 1 Hz was used in multiple flash experiments. After flashing, the samples were rapidly frozen (1−2 s) in cold ethanol (200 K) followed by storage in liquid nitrogen. The laser flash used was saturating under these conditions, in that the S_2 multiline signal formed by the flash was comparable in size to that formed in a similar sample by continuous illumination at 200 K.

Low-temperature illumination was done in an unsilvered dewar using either liquid N_2 (77 K) or a dry ice/ethanol bath (200 K). A time−course study monitoring signals arising from Q_A^- showed saturation after 25 min at 77 K (data not shown). Thus 77 K illumination was done for 30 min for all of the experiments. In some experiments FCCP (400 μM FCCP in DMSO) was added to the sample and incubated for 30 min at room temperature in complete darkness. Thawing steps during the study of the temperature dependence of electron transfer were performed either in an ethanol bath cooled to specific temperatures using liquid nitrogen or in a Bruker N_2 gas flow cryostat.

RESULTS

Thermoluminescence was used to estimate the amount of Q_B in our sample. The energetics and the reduction state of photosystem II can be monitored by thermoluminescence. In this method, a charge-separated state is formed by illumination given at room temperature followed by cooling or given at low temperature. Light emission is then recorded during controlled heating of the sample, when the thermal energy is sufficient to allow charge recombination reactions that repopulate the excited state chlorophyll (for a review see, e.g., ref *34*). Figure 1 shows the thermoluminescence recorded from PSII particles isolated from *T. elongatus* after a series of flashes was given at room temperature. The sample frozen in the dark (0f, Figure 1a) shows no emission. After one flash, an emission curve is observable with a maximum around 51 °C attributed to $S_2Q_B^-$ recombination (Figure 1b). The emission band seen after two flashes is bigger than after one flash and exhibits a maximum around 46 °C (Figure 1c). This shift to lower temperature and its amplitude are attributed to the $S_3Q_B^-$ recombination (*35*, *36*). After two or more flashes a shoulder appeared on the low-temperature side of the band. This arises from $S_{2/3}Q_A^-$ recombination, and this is the dominant reaction after 20 flashes (Figure 1f).

The thermoluminescence flash sequence provides information on the presence of Q_B and it redox state (*35*, *36*). The lack of a $S_2Q_A^-$ emission peak after one flash indicates that Q_B or Q_B^- is present in all centers. The relatively low intensity of thermoluminescence on the first flash compared to the second flash is indicative of a high concentration of Q_B^- present in the dark (*35*, *36*).

We attempted to diminish the concentration of Q_B^- present in the dark by longer dark adaptation at room temperature (up to 24 h). Some increase in the thermoluminescence on the first relative to the second flash occurred but not to the extent expected (not shown). EPR studies showed that this was due to the decay of $TyrD^{\bullet}$ during the dark adaptation

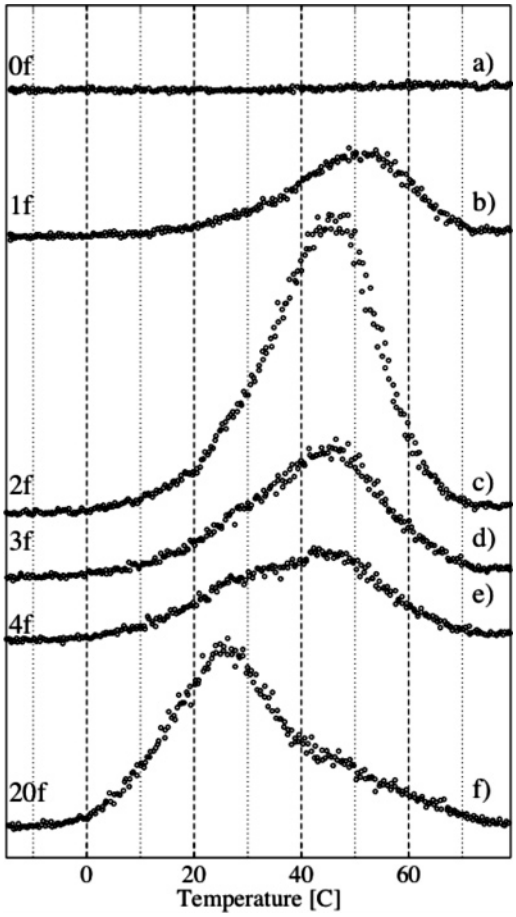

FIGURE 1: Thermoluminescence from short dark-adapted PSII particles (10 min) of *T. elongatus* after 0 (a), 1 (b), 2 (c), 3 (d), 4 (e), or 20 (f) flashes given at 20 °C.

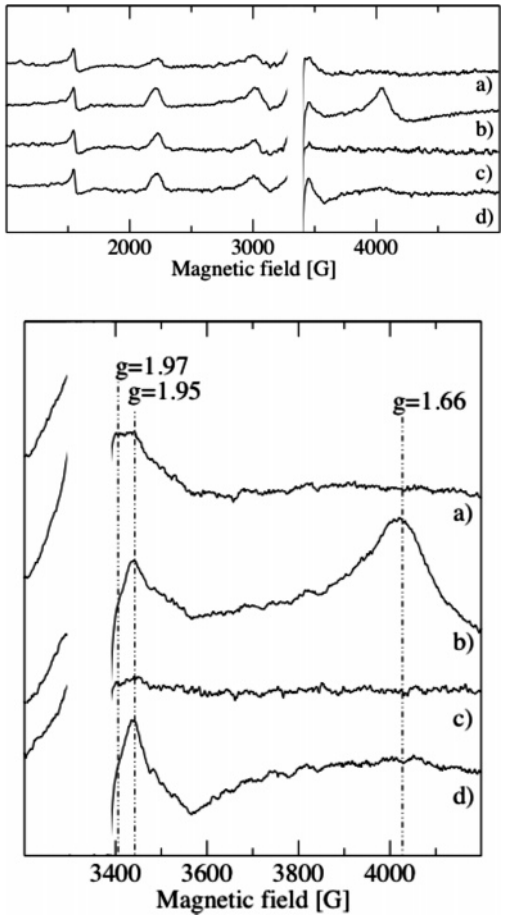

FIGURE 2: EPR spectra of PSII particles of *T. elongatus* after short (a) and long (c) dark adaptation and their corresponding spectra after illumination for 30 min at 77 K, (b) and (d), respectively. The upper panel shows a broad scan (one scan). The lower panel shows a magnification (five scans). Spectra were recorded at 5 K, microwave power 32 mW, and modulation amplitude 25 G.

(not shown but see below). The TyrD formed donates to S_2 and S_3 (*37*, *38*) and, thus, lowers the thermoluminescence intensities.

Figure 2 shows EPR spectra of PSII with the four upper traces recorded using a wide-field scan. The spectra show the following features: (1) the ubiquitous, so-called "junk" non-heme Fe^{3+} signal around 1500 G; (2) the g_x and g_y signals of low-spin heme Fe^{3+} at approximately 2200 and 3050 G from cytochrome c_{550} (cyt c_{550}) and cytochrome b_{559} (cyt b_{559}); (3) a gap in the spectrum around 3350 G ($g \approx 2$) where the intense narrow signals from the organic free radicals ($TyrD^{\bullet}$ in all samples and some Car^{+} and $ChlZ^{+}$ after illumination) are off scale; (4) a region higher than 3350 G that shows changes attributable to the semiquinone−iron complex, which is expanded in the lower panel.

Figure 2a shows that, in a PSII sample dark-adapted for a short period, an EPR signal is present at $g = 1.95$ with a shape similar to those attributed to semiquinone−iron complexes in PSII (*21*, *24*). In a sample dark-adapted for a longer time at room temperature this signal disappeared (Figure 2c). From the stability of the signal and the correlation to the thermoluminescence, it seems likely that this signal arises from $Fe^{2+}Q_B^{-}$ (*21*−*23*). This assignment is confirmed below.

Scans b and d of Figure 2 show the EPR spectra obtained when the PSII samples were illuminated at 77 K, a treatment that results in the formation of Q_A^{-} in most of the centers. The electron transferred to Q_A originates mainly from the side-path donors, β-carotene (Car), cytochrome b_{559} (cyt b_{559}), and chlorophyll Z (ChlZ) (*39*, *40*). Indeed, the wide-field scans in the upper part of Figure 2 show increases in the low-spin heme signals, reflecting cyt b_{559} oxidation. Increases in the $g = 2$ region reflect electron donation from Car and ChlZ in the fraction of centers where the cyt b_{559} is oxidized prior to illumination (not shown but see below). The high quantum yield electron donation from TyrZ, which has been recently reported to occur in the S_1 and S_0 states at liquid helium temperature (*41*; see also ref *42*), is thought to occur at 77 K; however, illumination for a long period, as used in the present study, appears to favor the more stable side-path electron donor pathway (*41*).

When Q_A^{-} is generated by illumination at 77 K in the long dark-adapted sample (Figure 2d), an EPR signal appears close to $g = 1.95$ that is attributable to $Q_A^{-}Fe^{2+}$ (*24*). In the sample adapted in darkness for a short time (Figure 2a), the formation of Q_A^{-} by 77 K illumination (Figure 2b) slightly decreases the intensity and changes the shape of the EPR signal around $g = 1.95$, with a marked loss of intensity at $g = 1.97$. The most marked effect, however, is the appearance of a relatively strong signal at $g = 1.66$. This signal has been attributed to $Q_A^{-}Fe^{2+}Q_B^{-}$ (*26*), and this assignment corresponds to the expected state in the present sample.

Figure 3 shows the EPR spectra recorded at 10 K in samples given zero to three flashes at room temperature

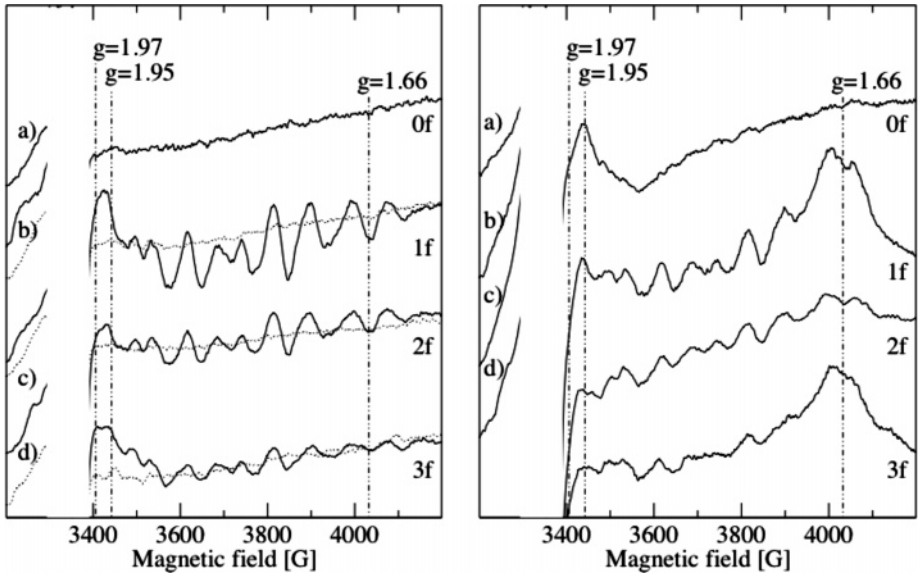

FIGURE 3: Flash sequence of long dark-adapted PSII particles of *T. elongatus* (left panel) and their corresponding spectra after illumination for 30 min at 77 K (right panel). The samples were given 0 (a), 1 (b), 2 (c), or 3 (d) flashes at room temperature and rapidly frozen. The spectra of each sample prior to flashes are shown as dotted lines. Spectra were recorded at 10 K, microwave power 32 mW, five scans, and modulation amplitude 25 G.

(Figure 3a−d, solid lines, left panel). The EPR spectra of the one and three flash samples showed a signal around $g = 1.95$ (Figure 3b,d, left panel). This signal was absent in the dark sample (Figure 3a) and small after two flashes (Figure 3c, left). This damped period-of-two oscillation in the intensity of the $g = 1.95$ signal is evidence that this signal arises from Q_B^-. This signal, however, overlaps with the multiline signal, arising from the S_2 state of the oxygen evolving complex.

The right panel of Figure 3 shows the effect of 77 K illumination on the samples of the flash series (left panel). The one and three flash samples show the signal at $g = 1.66$ (Figure 3b,d, right panel), while it is absent in the zero flash sample and weak in the two flash sample. Here again the damped period-of-two oscillation in the intensity of the $g = 1.66$ signal (from $Q_A^-Fe^{2+}Q_B^-$) supports the assignment of the $g = 1.95$ signal to the $Fe^{2+}Q_B^-$ state.

The flash experiments shown in Figure 3 indicate the presence of more than one exchangeable quinone in the preparation.

The comparison of the left and right panels of Figure 3 shows that the amplitude of the flash-induced S_2 multiline signal is significantly decreased by the 77 K illumination. This is attributed to the effect of infrared radiation (present in white light used for illumination at 77 K), which is absorbed by the Mn cluster, converting the spin $= {}^1/_2$ multiline state to a higher spin state that is trapped at low temperature (*43*, *44*).

In the flash experiment shown in the left planel of Figure 3 the S_2 Mn multiline signal is generated by the first flash. Its intensity decreases upon the second and third flashes. These flash-induced changes in intensity of the S_2 signal are less well defined than reported earlier in PSII from this species (*31*). This is to be expected in the present experiment for a number of reasons: (1) no added artificial electron acceptor could be used, (2) the standard preflash treatment for synchronizing the S states could not be applied, and (3) the long dark adaptation needed to eliminate Q_B^- led to the reduction of TyrD which is able to donate to S_2 and S_3 (not shown but see Figure 5).

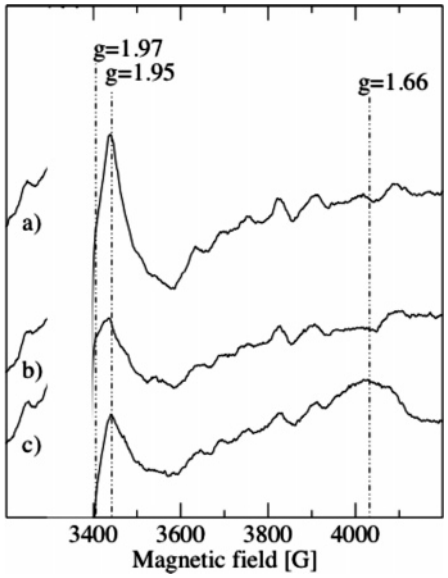

FIGURE 4: EPR spectra of *T. elongatus* PSII particles (dark-adapted for 15 h) after a low-temperature illumination and subsequent warming cycle. The sample was illuminated for 30 min at 77 K (a), thawed for 20 s to room temperature (b), and then reilluminated for 30 min at 77 K (c). The spectra were recorded at 10 K, microwave power 32 mW, five scans, and modulation amplitude 25 G.

As the S_2 multiline EPR signal from the Mn cluster overlaps the semiquinone−iron signals shown in the flash experiment of Figure 3, we attempted to generate Q_B^- under conditions where the formation of the S_2 state was minimized. Figure 4 shows the EPR spectra obtained by an experiment in which dark-adapted samples were illuminated at 77 K. The state formed has $Q_A^-Fe^{2+}$ in most centers, as manifest by the EPR signal at $g = 1.95$ (Figure 4a), with the electrons coming from the side pathway involving cyt b_{559}, Car, and ChlZ. When the sample was warmed in darkness to room temperature for 20 s and refrozen, the

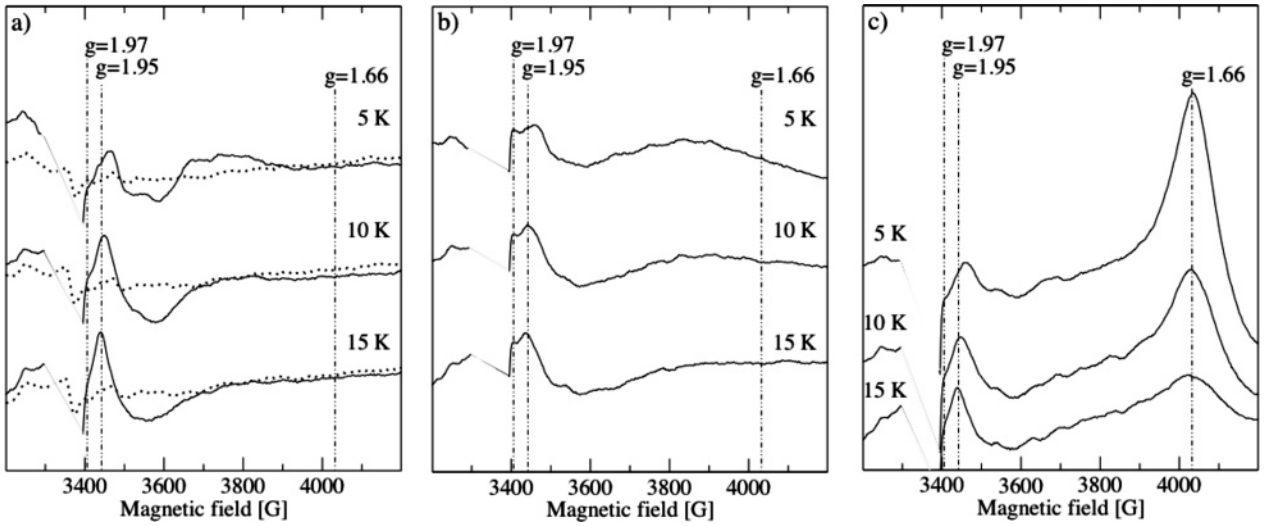

FIGURE 5: EPR spectra of *T. elongatus* PSII particles (dark-adapted for 15 h) after incubation with FCCP (400 μM, 30 min) in complete darkness. (a) Dotted lines show dark-adapted samples while the solid line shows the $Q_A^-Fe^{2+}$ signal induced by 77 K illumination for 30 min, (b) the $Fe^{2+}Q_B^-$ signal induced by a flash given at room temperature, and (c) same as (b) with an additional illumination at 77 K for 30 min. Spectra were taken at 5, 10, and 15 K. EPR settings: five scans, modulation amplitude 25 G, and microwave power 32 mW.

spectrum in Figure 4b was obtained. The warming step should have allowed electron transfer from Q_A^- to Q_B to occur, and indeed the spectrum gets broader with increased intensity at $g = 1.97$; this feature is attributed to $Fe^{2+}Q_B^-$. This spectrum is similar to that obtained in the flash experiments (Figure 3) and to the signal present in the short dark-adapted sample (Figure 2a). This experiment is similar to those done previously in which an $Fe^{2+}Q_B^-$ signal was first reported in plant PSII (*21*, *22*).

The sample illuminated at 77 K to form Q_A^- (Figure 4a) and then thawed to allow electron transfer from Q_A^- to Q_B (Figure 4b) was then given an additional illumination at 77 K, resulting in the spectrum shown in Figure 4c. A signal at $g = 1.66$ was formed by this treatment. The size of this signal is proportional to the Q_B^- formed by electron transfer from Q_A^- to Q_B upon the thawing step. The amplitude of the $g = 1.66$ EPR signal in Figure 4 is smaller than that shown in Figures 2 or 3. This implies that some Q_A^- is lost by charge recombination rather than by forward electron transfer upon the warming step. Additional thawing results in the loss of the $Q_A^-Fe^{2+}Q_B^-$ $g = 1.66$ signal, presumably either due to the electron transfer from Q_A^- to Q_B^- forming plastoquinol, Q_BH_2, or due to recombination of Q_A^-. A third illumination at 77 K regenerated a fraction of the $g = 1.66$ signal, indicating that on the thawing step at least some of the Q_A^-, which was formed by the 77 K illumination, decayed by charge recombination rather than by forward electron transfer (data not shown but see below).

A second approach for obtaining the $Fe^{2+}Q_B^-$ signal in the absence of the S_2 Mn multiline signal is to use an external electron donor to reduce the S_2 state back to the S_1 state after the flash. FCCP has been used to do this in optical studies of Q_B function in the past (*45*). Figure 5a (dotted line) shows the EPR spectra of a sample incubated for 30 min in the dark with FCCP. Figure 5b shows the EPR spectra of a sample that was given a single flash in the presence of FCCP. A signal around $g = 1.95$ was formed that is attributable to $Fe^{2+}Q_B^-$. Again, the signal is virtually identical those attributed to $Fe^{2+}Q_B^-$ generated under the different conditions described above (Figures 2−4). Here again, the illumination at 77 K induces the formation of the $g = 1.66$ signal (Figure 5c), while illumination of the zero flash sample (Figure 5a, dotted line) induces the formation of a $g = 1.95$ signal (Figure 5a, solid line) which is attributed to $Q_A^-Fe^{2+}$.

Given the lack of overlap with other signals and the relatively high yields of the states in the FCCP-containing sample, we studied the effect of temperature on the shape of the semiquinone−iron signals. Figure 5 shows the $Q_A^-Fe^{2+}$, $Fe^{2+}Q_B^-$, and the $Q_A^-Fe^{2+}Q_B^-$ signals recorded at 5, 10, and 15 K.

The $Q_A^-Fe^{2+}$ signal (Figure 5a, solid lines) consists of a peak that is temperature dependent ($g = 1.93$ at 5 K; $g = 1.95$ at 10/15 K) and a trough at higher field (peak to trough ~100 G). The $Fe^{2+}Q_B^-$ signal (Figure 5b) exhibits a similar temperature-dependent peak ($g = 1.93$ at 5 K; $g = 1.95$ at 10/15 K), but in addition it shows an apparently temperature-independent feature at $g = 1.97$. The $Fe^{2+}Q_B^-$ signal also shows a trough at higher field (peak to trough ~100 G), but it has a somewhat broader shape than that of $Q_A^-Fe^{2+}$. The amplitude of the $Q_A^-Fe^{2+}$ signal shows a slightly more marked increase with temperature than does the $Fe^{2+}Q_B^-$ signal. The spectrum in Figure 5c exhibits features at $g = 1.66$ and $g = 1.95$. The $g = 1.66$ signal is attributed to $Q_A^-Fe^{2+}Q_B^-$. The signal increase as the temperature is lowered and its g-value seem to be constant. The $g = 1.95$ signal in Figure 5c shows the same temperature behavior in terms of its g-value and its size as the $Q_A^-Fe^{2+}$ signal (Figure 5a). It is attributed to $Q_A^-Fe^{2+}$ generation in centers lacking the $Fe^{2+}Q_B^-$ state.

It is of note that in this experiment we expected FCCP to donate to the flash-induced S_2 state, resulting in formation of S_1. Instead, we found that in our conditions FCCP was a rather slow electron donor to S_2, and increasing the concentration of FCCP led to the loss of $TyrD^{\bullet}$. Under the conditions of the experiment shown in Figure 5, FCCP incubation had virtually eliminated the $TyrD^{\bullet}$ prior to the flash (see Figure 5a, dotted line). After the flash, the S_2 Mn multiline signal was absent but the $TyrD^{\bullet}$ signal was generated in a fraction of the centers. Thus the FCCP eliminated the S_2 state, and hence the multiline signal, but it did so at least in part by

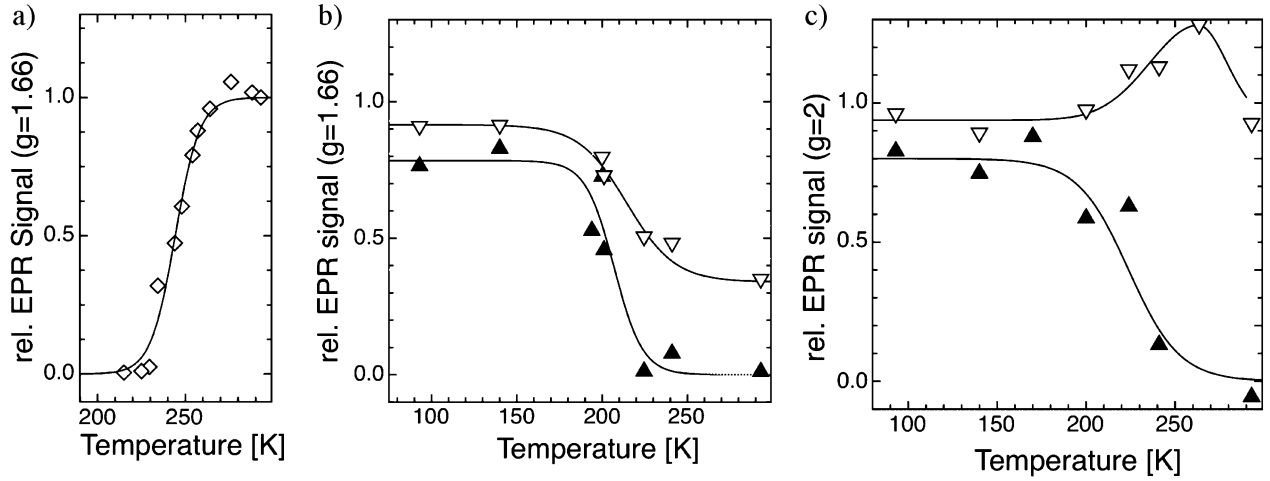

FIGURE 6: Temperature dependence of the electron transfer from Q_A^- to Q_B (a) and from Q_A^- to Q_B^- (b). The first electron transfer step (a) was monitored by the appearance of the $g = 1.66$ EPR signal after an additional illumination. The second electron transfer step (b) was monitored by the disappearance of the $g = 1.66$ EPR signal (filled triangles). This disappearance is caused by the forward electron transfer and by charge recombination involving Q_A^-. The charge recombination partner of Q_A^- is $Car^+/ChlZ^+$ (c, filled triangles). To discriminate forward electron transfer from charge recombination, an additional illumination regenerated a fraction of the $g = 1.66$ signal, resulting in the temperature dependency of the second electron transfer step from Q_A^- to Q_B^- (b, open triangles). This additional illumination also increased the radical at $g = 2$ (c, open triangles). EPR spectra were recorded at 5 K with a microwave power of 32 mW and modulation amplitude of 25 G (a, b) or at 15 K with a microwave power of 2 μW and modulation amplitude of 3 G (c).

prereducing the $TyrD^\bullet$ forming TyrD, which acted as an electron donor to S_2 (*37*, *38*).

In the following experiments we used the $g = 1.66$ signal from the $Q_A^-Fe^{2+}Q_B^-$ state to investigate the temperature dependence of electron transfer between the quinones in PSII. The temperature dependence of the first electron transfer step from Q_A^- to Q_B was investigated by the following protocol. First the Q_A^- state was generated by 30 min illumination at 77 K. Then the sample was warmed to a given temperature for 30 s to allow electron transfer to Q_B. The samples were reilluminated at 77 K for 30 min to regenerate Q_A^-, thereby generating the $g = 1.66$ signal (the $Q_A^-Fe^{2+}Q_B^-$ state) in any centers having Q_B^-. In this experiment then the amplitude of the $g = 1.66$ signal is proportional to the centers in which an electron transfer from Q_A^- to Q_B occurred during the warming step. Figure 6a shows the extent of the $g = 1.66$ signal versus the temperature of incubation. The yield of electron transfer from Q_A^- to Q_B was 50% at approximately −28 °C (245 K). No electron transfer occurred at −50 °C, while at −10 °C the electron transfer was complete.

The temperature dependence for the second electron transfer reaction from Q_A^- to Q_B^- was investigated by monitoring the loss of the $g = 1.66$ EPR signal (i.e., $Q_A^-Fe^{2+}Q_B^-$) after incubation at a given temperature. To generate the $g = 1.66$ signal, the samples were given a flash at room temperature to generate the $S_2Fe^{2+}Q_B^-$ state, followed by illumination at 77 K for 30 min to form the $Q_A^-Fe^{2+}Q_B^-$ state. The samples were then warmed and incubated for 30 s at a given temperature. Figure 6b (filled triangles) shows the results of such an experiment. About 20% of the $Q_A^-Fe^{2+}Q_B^-$ signal was already lost at the lowest incubation temperature, presumably due to charge recombination occurring at low temperatures in a fraction of centers. In the majority of centers, however, the temperature at which the $g = 1.66$ signal decreased by 50% was approximately −63 °C (210 K).

Since loss of the $Q_A^-Fe^{2+}Q_B^-$ state in the experiment in Figure 6b could occur either by forward electron transfer or by charge recombination, the samples were measured not only before (the 100% value) and after the warming step (solid triangles) but also after an additional period of illumination at 77 K (open triangles). This additional illumination should regenerate the $Q_A^-Fe^{2+}Q_B^-$ state (i.e., $g = 1.66$ signal) in those reaction centers where Q_A^- had decayed due to charge recombination rather than by forward electron transfer. These data should reflect the temperature dependence of the Q_A^- to Q_B^- electron transfer step without interference from charge recombination. The temperature at which this reaction is half-complete is −58 °C (215 K), does not occur at temperatures below approximately 180 K, and is complete at 250 K.

In the experiments of Figure 6b the increase in the $Q_A^-Fe^{2+}Q_B^-$ signal after the second illumination (open triangles) compared to that measured directly after the warming period (closed triangles) mainly reflects the centers in which Q_A^- decayed by recombination during the warming period. The data indicate the presence of two different recombination reactions: (1) in about 20% of the measured centers recombination occurred already at the lowest incubation temperature used (93 K); (2) in the other fraction of the measured centers, recombination occurred at temperatures higher than 220 K. However, the $Q_A^-Fe^{2+}Q_B^-$ signal generated by the second illumination after warming to temperatures high enough to allow Q_A^- to Q_B electron transfer is expected to contain a contribution from those centers in which Q_B was not reduced by the laser flash. Such centers, representing the "photochemical miss factor" [8% in this material (*46*)], were expected to contain Q_A^- after the first illumination at 77 K and to undergo electron transfer upon warming, forming Q_B^- which appears then as the $Q_A^-Fe^{2+}Q_B^-$ signal after the second illumination at 77 K.

To determine the recombination partner for Q_A^- as measured by the decay of the $g = 1.66$ signal during the warming step, we followed the EPR signals of the Car/ChlZ radicals in the $g = 2$ region and the cytochrome ($g = 3.0$) looking for a temperature-dependent behavior comparable to that seen for the $g = 1.66$ signal. The proportion of cyt

b_{559} already oxidized prior to low-temperature illumination varied between 30% and 50% depending on the preparation. The cyt b_{559} that was reduced in the dark underwent oxidation upon illumination at 77 K, and as expected it remained stable upon warming. However, the radical signal from Car/ChlZ behaved as the recombination partner for the electron on Q_A^-.

Figure 6c shows the influence of warming on the intensity of the Car/ChlZ radical EPR signal generated by 77 K illumination. Warming to 93 K diminished the Car/ChlZ ($g = 2$) radical by approximately 20%, corresponding to about 10% of all centers (based on comparison to the $TyrD^\bullet$ signal measured after flash illumination). Reillumination at 77 K of the sample warmed to temperatures of 180 K and below regenerated the radical to almost the level seen with the first illumination at 77 K. Warming of the sample to 293 K resulted in complete loss of the Car/ChlZ radical signal. The range of temperature over which the Car/ChlZ radical decayed was comparable to that seen for decay of the $g = 1.66$ signal (Figure 6b).

Reillumination at 77 K of samples warmed to temperatures between 180 and 250 K resulted in an increase in the amplitude of the Car/ChlZ radical to a level 25% higher than was originally generated by the first 77 K illumination. This increase in the Car/ChlZ radical is expected in centers in which cyt b_{559} is the origin of the electron trapped on Q_A^- on the first 77 K illumination and where Q_A^- decays by forward electron transfer upon warming. The temperature dependence of this increase is comparable to the temperature dependence of forward Q_A^- to Q_B^- electron transfer measured by the decay of the $Q_A^-Fe^{2+}Q_B^-$ state, shown in Figure 6b.

DISCUSSION

We report here the X-band EPR spectra of $Fe^{2+}Q_B^-$ and $Q_A^-Fe^{2+}Q_B^-$ in PSII from *T. elongatus*. The signals are similar to those attributed to these states earlier (see introduction). However, the assignments here are much more firm since both signals exhibit period-of-two, flash-dependent variations in intensity. This behavior is the definitive characteristic of Q_B function (*4*, *5*). The EPR signal from $Fe^{2+}Q_B^-$ is similar to that of $Q_A^-Fe^{2+}$, but they can be distinguished from each other in terms of their temperature dependence and shape (see Figures 2−5). The dominant feature of both states is at $g = 1.95$, but the $Fe^{2+}Q_B^-$ signal shows additional intensity around $g = 1.97$.

Because it is relatively intense and it is at a field position that has little overlap with other signals, the $g = 1.66$ signal has already been used as a probe for the presence of Q_B^-. The $g = 1.66$ signal was used to estimate the redox potential of Q_B (26), to show the involvement of Q_A^- in charge recombination with a low-temperature-generated radical pair thought to involve $TyrZ^\bullet$ (*41*), and to detect the presence of Q_B^- in thylakoids membranes where other semiquinone−iron signals were obscured by overlapping signals (23). Here we investigated the temperature dependence of the electron transfer from Q_A^- to Q_B and from Q_A^- to Q_B^-. Under the conditions of our experiment (30 s of incubation at the test temperature), the temperature at which Q_A^- to Q_B electron transfer occurred in half of the centers was around −28 °C (245 K). No electron transfer occurred at −50 °C, while at −10 °C the transfer was complete. For the Q_A^- to Q_B^- step the values were less precise but the temperature for transfer to occur in half of the centers was around −58 °C (215 K), the transfer did not occur at temperatures below approximately −93 °C (180 K), and the transfer was complete at −23 °C (250 K) and above. Clearly, the Q_A^- to Q_B transfer step is frozen out at a temperature 30 °C higher than the Q_A^- to Q_B^- step. In addition, temperature-induced inhibition appears to occur over a narrower temperature range for the first step compared to the second. These results indicate that the reactions may have quite different limiting steps. These results agree well with an earlier study done on PSII-enriched membranes from spinach (*17*) using fluorescence to monitor Q_A^- decay (see below).

Our experiment aimed at determining the temperature dependence of Q_A^- to Q_B^- electron transfer is rendered more complicated by heterogeneity on the electron donor side. At 77 K long illumination results in oxidation of Car, ChlZ, and cyt b_{559}, the side-path electron donors, in most centers. In a large fraction of centers electron donation occurs from cyt b_{559}. The oxidized cyt b_{559} does not participate in charge recombination reactions; thus the Q_A^- formed is expected to be stable until it undergoes forward electron transfer. However, where the cyt b_{559} is already oxidized, the charge localizes on Car/ChlZ.

In a small fraction of centers Q_A^- is lost due to recombination at temperatures lower than 93 K. It seems likely that this reflects a fraction of centers where the positive charge remains localized on the Car rather than being transferred to ChlZ (*39*, *40*), but a definitive assignment requires the use of other methods to distinguish between Car and Chl radicals (*39*, *40*, *47*).

The $ChlZ^+Q_A^-$ charge pair appears to recombine with a yield of 50% during 30 s at about 220 K. This transition occurs at almost the same temperature as the forward electron transfer, Q_A^- to Q_B^-. It seems very likely that, in centers in the $ChlZ^+Q_A^-$ state, both the forward reaction and the back-reaction compete. Given that the forward reaction is so different to the back-reaction, the similar temperature dependence might not be a coincidence. The whole system might undergo a phase transition (solvent/protein) making both reactions possible at the same temperature.

However, further experiments are required before a complete picture of the events occurring during the warming step is obtained. In this regard, a more native sample, in which a greater quantity of the cyt b_{559} is in its high-potential form and is therefore reduced before illumination, would simplify the situation. In such a sample a greater proportion of centers would be predicted to undergo forward electron transfer rather than recombination under the conditions of this experiment. This is, however, technically difficult as the cyt b_{599} component is easily oxidized during the preparation.

In the literature the temperature dependence of electron transfer between Q_A and Q_B has been studied using fluorescence methods. In plant PSII membranes the Q_A^- to Q_B step was shown to be thermally blocked with a half-maximum effect at close to −20 °C (*17*). This value is in good agreement with that reported here. In the same study it was also found that Q_A^- to Q_B^- electron transfer appeared to occur at lower temperatures, being still functional in a significant fraction of the centers at the lowest temperature tested (−55 °C). This is also consistent with the more detailed

study we report here where this temperature is close to the half-maximum effect.

In earlier studies using plant chloroplasts, fluorescence decay reflecting forward electron transfer from Q_A^- was reported to occur slowly at −60 °C. This is lower than we see here for Q_A^- to Q_B. However, since short dark-adapted chloroplasts are known to contain around 20−40% of Q_B^- stable in the dark (*4*, *18*, *48*, *49*), it is likely that the Q_A^- decay reported would reflect Q_A^- to Q_B^- electron transfer. This report of forward electron transfer at −60 °C is thus consistent with our results. In the same work and in thermoluminescence studies (*50*) multiple turnovers (up to 6−7 electrons) were reported at −30 and −20 °C, respectively. This may also be consistent with the present work since both steps function at least partially at these temperatures.

The temperature at which the Q_A^- to Q_B electron transfer step is half-blocked is approximately 30 °C higher than that for the Q_A^- to Q_B^- electron transfer step. Since the temperature range over which the Q_A^- to Q_B^- step is thermally blocked seems broader, some Q_A^- to Q_B^- electron transfer still occurs at surprisingly low temperatures. For example, Q_A^- to Q_B^- electron transfer still occurs in a significant fraction of centers at 200 K, a temperature that is often used for illumination of PSII on the tacit assumption that a single turnover takes place. This will be so in all of the centers only when Q_B^- is absent prior to illumination.

It has been demonstrated that the Q_A^- to Q_B electron transfer is faster than that from Q_A^- to Q_B^- (*15*, *16*, *18*). This also is the case in the homologous bacterial reaction center (*13*, *14*; see, however, ref *51*). In PSII the temperature dependence of both of these rates has not been studied in detail (*17*, *52*). The finding that the slower of the two steps at room temperature (i.e., the Q_A^- to Q_B^-) continues to function at a much lower temperature than the faster of the steps (Q_A^- to Q_B) is something of a surprise and is a further indication that there is a significant difference in the nature of the reactions occurring.

In the purple bacterial reaction center the equivalent electron transfer steps are quite different from each other in terms of the reactions that limit their rate (for a review see ref *13*). The first electron transfer Q_A^- to Q_B is controlled by a gating mechanism (*53*) while the Q_A^- to Q_B^- is limited by protonation events (*54*). The nature of the gating mechanism is the subject of some debate (*53*−*58*). By comparing the structures obtained from crystals that were dark-adapted versus those that were frozen under illumination, the movement of Q_B was proposed to be the gating event (*55*). A number of recent studies, however, have seriously questioned this idea (*56*, *57*). These studies indicate that Q_B is in the so-called proximal site even in the dark (*56*, *57*). If so, the nature of the gating mechanism remains to be determined. Whatever the nature of the gating mechanism is, it seems quite likely that a similar event occurs in PSII (*17*, *59*). The temperature dependence of the electron transfer steps is consistent with such a gating mechanism in PSII. A marked change in the flexibility of the ligand environment of the iron, as measured by Mössbauer spectroscopy, was found to occur over the temperature range at which the Q_A^- to Q_B transfer step was frozen out in bacterial reaction centers (*60*) and PSII (*59*). This could reflect an aspect of the putative gating mechanism. In purple bacterial reaction centers the gating mechanism was demonstrated by substituting Q_A with quinones of different potential (*53*). The change in the driving force had no influence on the Q_A^- to Q_B step. Comparable direct evidence for a gating mechanism in PSII has yet to be reported.

NOTE ADDED IN PROOF

Earlier this year Kern et al. (*61*) reported 2.9 ± 0.8 plastoquinones per isolated PSII from *T. elongatus*, which is consistent with our interpretation of our data that more than one exchangeable quinone is isolated with the reaction center.

ACKNOWLEDGMENT

We thank Drs. J. Lavergne, J. Breton, A. Boussac, J.-M. Ducruet, and D. Kirilovsky for very helpful discussion. We also thank Dr. M. Sugiura for the His tag strain of *T. elongatus* and D. Kirilovsky for help and advice in the growth of this strain and the isolation and purification of the protein. Finally, we thank J.-M. Ducruet for help and advice on the thermoluminescence measurements.

REFERENCES

1. Diner, B. A., and Babcock, G. T. (1996) Structure, dynamics, and energy conversion efficiency in photosystem II, in *Oxygenic Photosynthesis: The Light Reactions* (Ort, D. R., and Yocum, C. F., Eds.) pp 213−247, Kluwer, Dordrecht.
2. Rutherford, A. W. (1989) Photosystem II, the water-splitting enzyme, *Trends Biochem. Sci. 14*, 227−232.
3. Crofts, A. R., and Wraight, C. A. (1983) The electrochemical domain of photosynthesis, *Biochim. Biophys. Acta 726*, 149.
4. Bouges-Bocquet, B. (1973) Electron transfer between the two photosystems in spinach chloroplasts, *Biochim. Biophys. Acta 314*, 250−256.
5. Velthuys, B. R., and Amesz, J. (1974) Charge accumulation at the reducing side of system 2 of photosynthesis, *Biochim. Biophys. Acta 333*, 85.
6. Wraight, C. A. (1981) Oxidation−reduction physical chemistry of the acceptor quinone complex in bacterial photosynthetic reaction centers: Evidence for a new model of herbicide activity, *Isr. J. Chem. 21*, 348−354.
7. Velthuys, B. R. (1981) Electron-dependent competition between plastoquinone and inhibitors for binding to photosystem II, *FEBS Lett. 126*, 277−281.
8. Michel, H., and Deisenhofer, J. (1988) Relevance of the photosynthetic reaction center from purple bacteria to the structure of photosystem II, *Biochemistry 27*, 1−7.
9. Zouni, A., Witt, H. T., Kern, J., Fromme, P., Krauss, N., Saenger, W., and Orth, P. (2001) Crystal structure of photosystem II from *Synechococcus elongatus* at 3.8 Å resolution, *Nature 409*, 739−743.
10. Ferreira, K. N., Iverson, T. M., Maghlaoui, K., Barber, J., and Iwata, S. (2004) Architecture of the photosynthetic oxygen-evolving center, *Science 303*, 1831−1838.
11. Hoff, A. J. (1993) Magnetic resonance of bacterial photosynthetic reaction centers, in *The Photosynthetic Reaction Center* (Deisenhofer, J., and Norris, J. R., Eds.) pp 331−386, Academic Press, San Diego.
12. Rutherford, A. W. (1986) How close is the analogy between the reaction centre of photosystem II and that of purple bacteria?, in *Progress in Photosynthesis Research* (Biggins, J., Ed.) pp 277−283, Kluwer, Dordrecht.
13. Okamura, M. Y., Paddock, M. L., Graige, M. S., and Feher, G. (2000) Proton and electron transfer in bacterial reaction centers, *Biochim. Biophys. Acta 1458*, 148−163.
14. Wraight, C. A. (2004) Proton and electron transfer in the acceptor quinone complex of photosynthetic reaction centers from *Rhodobacter sphaeroides*, *Front. Biosci. 9*, 309−337.
15. Bowes, J. M., and Crofts, A. R. (1980) Binary oscillations in the rate of reoxidation of the primary acceptor of photosystem II, *Biochim. Biophys. Acta 590*, 373−384.

16. Robinson, H. H., and Crofts, A. R. (1983) Kinetics of the oxidation−reduction reactions of the photosystem II quinone acceptor complex, and the pathway for deactivation, *FEBS Lett. 153*, 221.
17. Reifarth, F., and Renger, G. (1998) Indirect evidence for structural changes coupled with Q_B^-. Formation in photosystem II, *FEBS Lett. 428*, 123−126.
18. de Wijn, R., and van Gorkom, H. J. (2001) Kinetics of electron transfer from Q_A to Q_B in photosystem II, *Biochemistry 40*, 11912−11922.
19. Crofts, A. R., Robinson, H. H., and Snozzi, M. (1984) Reactions of quinones at catalytic sites; A diffusional role in H-transfer, in *Advances in Photosynthesis Research* (Sybesma, C., Ed.) pp 461−468, N. Martinus and W. Junk (Kluwer), The Hague.
20. Berthold, D. A., Babcock, G. T., and Yocum, C. F. (1981) A highly resolved, oxygen-evolving photosystem II preparation from spinach thylakoid membranes: EPR and electron-transport properties, *FEBS Lett. 134*, 231−234.
21. Rutherford, A. W., Zimmermann, J.-L., and Mathis, P. (1984) EPR of PS II-interactions, herbicide effects and a new signal, in *Advances in Photosynthesis Research* (Sybesma, C., Ed.) pp 445−448, N. Martinus and W. Junk (Kluwer), The Hague.
22. Zimmermann, J.-L., and Rutherford, A. W. (1986) Photoreductant-induced oxidation of Fe^{2+} in the electron-acceptor complex of photosystem II, *Biochim. Biophys. Acta 851*, 416−423.
23. Hallahan, B. J., Ruffle, S. V., Bowden, S. J., and Nugent, J. H. A. (1991) Identification and characterisation of EPR signal involving Q_B semiquinone in plant photosystem II, *Biochim. Biophys. Acta 1059*, 181−188.
24. Rutherford, A. W., and Zimmermann, J. L. (1984) A new EPR signal attributed to the primary plastosemiquinone acceptor in photosystem II, *Biochim. Biophys. Acta 767*, 168−175.
25. McDermott, A. E., Yachandra, V. K., Guiles, R. D., Cole, J. L., Dexheimer, S. L., Britt, R. D., Sauer, K., and Klein, M. P. (1988) Characterization of the manganese O_2-evolving complex and the iron-quinone acceptor complex in photosystem II from a thermophilic cyanobacterium by electron paramagnetic resonance and X-ray absorption spectroscopy, *Biochemistry 27*, 4021−4031.
26. Corrie, A. R., Nugent, J. H. A., and Evans, M. C. W. (1991) Identification of EPR signals from the $Q_A^{\bullet-}Q_B$ and $Q_B^{\bullet-}$ in photosystem II from *Phormidium laminosum*, *Biochim. Biophys. Acta 1057*, 384−390.
27. Kuhl, H., Krieger, A., Seidler, A., Boussac, A., Rutherford, A. W., and Rögner, M. (1998) Characterisation and functional studies on a new photosystem II preparation from the thermophilic cyanobacterium *Synechococcus elongatus*, in *Photosynthesis: Mechanisms and Effects* (Garab, G., Ed.) pp 1001−1004, Kluwer, Dordrecht.
28. Boussac, A., Kuhl, H., Ghibaudi, E., Rogner, M., and Rutherford, A. W. (1999) Detection of an electron paramagnetic resonance signal in the S_0 state of the manganese complex of photosystem II from *Synechococcus elongatus*, *Biochemistry 38*, 11942−11948.
29. Zouni, A., Witt, H. T., Kern, J., Fromme, P., Krauss, N., Saenger, W., and Orth, P. (2001) Crystal structure of photosystem II from *Synechococcus elongatus* at 3.8 Å resolution, *Nature 409*, 739−743.
30. Sugiura, M., and Inoue, Y. (1999) Highly purified thermo-stable oxygen-evolving photosystem II core complex from the thermophilic cyanobacterium *Synechococcus elongatus* having His-tagged CP43, *Plant Cell Physiol. 40*, 1219−1231.
31. Boussac, A., Rappaport, F., Carrier, P., Verbavatz, J. M., Gobin, R., Kirilovsky, D., Rutherford, A. W., and Sugiura, M. (2004) Biosynthetic Ca^{2+}/Sr^{2+} exchange in the photosystem II oxygen-evolving enzyme of *Thermosynechococcus elongatus*, *J. Biol. Chem. 279*, 22809−22819.
32. Kirilovsky, D., Roncel, M., Boussac, A., Wilson, A., Zurita, J. L., Ducruet, J. M., Bottin, H., Sugiura, M., Ortega, J. M., and Rutherford, A. W. (2004) Cytochrome *c*550 in the cyanobacterium *Thermosynechococcus elongatus*: study of redox mutants, *J. Biol. Chem. 279*, 52869−52880.
33. Ducruet, J.-M. (2003) Chlorophyll thermoluminescence of leaf discs: simple instruments and progress in signal interpretation open the way to new ecophysiological indicators, *J. Exp. Bot. 54*, 2419.
34. Rappaport, F., Cuni, A., Xiong, L., Sayre, R. T., and Lavergne, J. (2005) Charge recombination and thermoluminescence in photosystem II, *Biophys. J.* (in press).
35. Rutherford, A. W., Crofts, A. R., and Inoue, Y. (1982) Thermoluminescence as a probe of photosystem II photochemistry. The origin of the flash-induced glow peaks, *Biochim. Biophys. Acta 682*, 457−465.
36. Rutherford, A. W., Renger, G., Koike, H., and Inoue, Y. (1984) Thermoluminescence as a probe of photosystem II. The redox and protonation states of the secondary acceptor quinone and the O_2-evolving enzyme, *Biochim. Biophys. Acta 767*, 548−556.
37. Velthuys, B. R., and Visser, J. W. M. (1975) The reactivation of EPR signal II in chloroplasts treated with reduced dichlorophenol-indophenol: evidence against a dark equilibrium between two oxidation states of the oxygen evolving system, *FEBS Lett. 55*, 109−112.
38. Babcock, G. T., and Sauer, K. (1973) Electron paramagnetic resonance signal II in spinach chloroplasts. I. Kinetic analysis for untreated chloroplasts, *Biochim. Biophys. Acta 325*, 483−503.
39. Faller, P., Fufezan, C., and Rutherford, A. W. (2005) Side-path electron donors: cytochrome b_{559}, chlorophyll Z and β-carotene, in *Photosystem II: The Water/Plastoquinone Oxido-Reductase in Photosynthesis* (Wydrzynski, T., and Satoh, K., Eds.) Chapter 15, Kluwer, Dordrecht.
40. Tracewell, C. A., Vrettos, J. S., Bautista, J. A., Frank, H. A., and Brudvig, G. W. (2001) Carotenoid photooxidation in photosystem II, *Arch. Biochem. Biophys. 385*, 61−69.
41. Zhang, C., Boussac, A., and Rutherford, A. W. (2004) Low-temperature electron transfer in photosystem II: a tyrosyl radical and semiquinone charge pair, *Biochemistry 43*, 13787−13795.
42. Nugent, J. H. A., Muhiuddin, I. P., and Evans, M. C. W. (2002) Electron transfer from the water oxidizing complex at cryogenic temperatures: the S_1 to S_2 step, *Biochemistry 41*, 4117−4126.
43. Boussac, A., Girerd, J. J., and Rutherford, A. W. (1996) Conversion of the spin state of the manganese complex in photosystem II induced by near-infrared light, *Biochemistry 35*, 6984−6989.
44. Boussac, A., Un, S., Horner, O., and Rutherford, A. W. (1998) High-spin states ($S >/= 5/2$) of the photosystem II manganese complex, *Biochemistry 37*, 4001−4007.
45. Lavergne, J. (1987) Optical-difference spectra of the S-state transitions in the photosynthetic oxygen-evolving complex, *Biochim. Biophys. Acta 894*, 91.
46. Isgandarova, S., Renger, G., and Messinger, J. (2003) Functional differences of photosystem II from *Synechococcus elongatus* and spinach characterized by flash induced oxygen evolution patterns, *Biochemistry 42*, 8929−8938.
47. Hanley, J., Deligiannakis, Y., Pascal, A., Faller, P., and Rutherford, A. W. (1999) Carotenoid oxidation in photosystem II, *Biochemistry 38*, 8189−8195.
48. Fowler, C. F. (1977) Proton translocation in chloroplasts and its relationship to electron transport between the photosystems, *Biochim. Biophys. Acta 459*, 351−363.
49. Wollman, F.-A. (1978) Determination and modification of the redox state of the secondary acceptor of photosystem II in the dark, *Biochim. Biophys. Acta 503*, 263−273.
50. Inoue, Y., and Shibata, K. (1978) Oscillation of thermoluminescence at medium-low temperature, *FEBS Lett. 85*, 193−197.
51. Ginet, N., Comayras, F., and Lavergne, J. (2004) in *Proceedings of the 13th International Congress on Photosynthesis* (Bruce, D., and van der Est, A., Eds.) Montréal, Canada.
52. Kanazawa, A., Kramer, D., and Crofts, A. R. (1992) Temperature dependence of PS2 electron transfer reactions measured by flash-induced fluorescence changes, in *Research in Photosynthesis* (Murata, N., Ed.) pp 131−134, Kluwer, Dordrecht.
53. Graige, M. S., Feher, G., and Okamura, M. Y. (1998) Conformational gating of the electron transfer reaction $Q_A^-Q_B \rightarrow Q_AQ_B$ in bacterial reaction centers of *Rhodobacter sphaeroides* determined by a driving force assay, *Proc. Natl. Acad. Sci. U.S.A. 95*, 11679−11684.
54. Graige, M. S., Paddock, M. L., Bruce, J. M., Feher, G., and Okamura, M. Y. (1996) Mechanism of proton-coupled electron transfer for quinone (Q_B) reduction in reaction centers of *Rb. sphaeroides*, *J. Am. Chem. Soc. 118*, 9005−9016.
55. Stowell, M. H., McPhillips, T. M., Rees, D. C., Soltis, S. M., Abresch, E., and Feher, G. (1997) Light-induced structural changes in photosynthetic reaction center: implications for mechanism of electron−proton transfer, *Science 276*, 812−816.
56. Breton, J. (2004) Absence of large-scale displacement of quinone Q_B in bacterial photosynthetic reaction centers, *Biochemistry 43*, 3318−3326.

57. Xu, Q., Baciou, L., Sebban, P., and Gunner, M. R. (2002) Exploring the energy landscape for Q_A^- to Q_B electron transfer in bacterial photosynthetic reaction centers: effect of substrate position and tail length on the conformational gating step, *Biochemistry 41*, 10021−10025.
58. Cherepanov, D. A., Krishtalik, L. I., and Mulkidjanian, A. Y. (2001) Photosynthetic electron transfer controlled by protein relaxation: analysis by Langevin stochastic approach, *Biophys. J. 80*, 1033−1049.
59. Garbers, A., Reifarth, F., Kurreck, J., Renger, G., and Parak, F. (1998) Correlation between protein flexibility and electron transfer from Q_A^- to Q_B in PSII membrane fragments from spinach, *Biochemistry 37*, 11399−11404.
60. Parak, F., Frolov, E. N., Kononenko, A. A., Mossbauer, R. L., Goldanskii, V. I., and Rubin, A. B. (1980) Evidence for a correlation between the photoinduced electron transfer and dynamic properties of the chromatophore membranes from *Rhodospirillum rubrum*, *FEBS Lett. 117*, 368−372.
61. Kern, J., Loll, B., Lüneberg, C., DiFiore, D., Biesiadka, J., Irrgang, K.-D., and Zouni, A. (2005) Purification, characterisation and crystallisation of photosystem II from *Thermosynechococcus elongatus* cultivated in a new type of photobioreactor, *Biochim. Biophys. Acta 1706*, 147−157.

BI051000K